Received: 14 April 2024 | Revised: 31 July 2024 | Accepted: 20 August 2024 | Published online: 4 September 2024

RESEARCH ARTICLE

Archives of Advanced Engineering Science
2024, Vol. 00(00) 1–9
DOI: 10.47852/bonviewAAES42023106

BON VIEW PUBLISHING

Analysis of the Effects of Wheel Spacers on the Roll Stability of the Vehicle

Glenn Xavier Vaz[1] and Zeinab El-Sayegh[1,*]

[1]*Department of Automotive and Mechatronics Engineering, Ontario Tech University, Canada*

Abstract: This paper aims to identify the impact of tire spacers on the vehicle's overall stability and subsequently the influence of various kinematic factors due to the induced vehicle's roll moment. The placement of the spacers was studied as a function of the arrangement of the spacers and was compared to a model without spacers. The outcome of this project would be to highlight the importance of spacers to reduce the roll within a vehicle and to provide an idea for the customer about what orientation will provide the best results from the spacers that they have installed. Using the CarSim software, we were able to develop different accurate models within the scope of this study. A series of these models were then simulated using simulation software on a variety of real-life conditions in order to predict the behavior of the vehicle under different conditions. These results were used to evaluate the handling characteristics of the vehicle and determine the ideal placement of spacers attached to the wheels in order to improve the vehicle's handling characteristics.

Keywords: wheel spacers, CarSim, fish hook test, roll angle, roll gradient, axle moment

1. Introduction

When a vehicle takes a turn, the rotation of a vehicle's body along its longitudinal axis, toward the outside of a turn is known as body roll. The forces acting on a vehicle during a turn are depicted in Figure 1 [1]. Body roll is the result of the suspension system's compliance, which permits the body of the car, which is supported by the suspension, to tilt in the direction of the centrifugal force pushing against the car. Equation (1) [2] is Euler's equation for the moment exerted along the longitudinal axis (M_x) on a vehicle with six degrees of freedom. The moment depends on the inertia ($I_{1,2,3}$), roll rate (ω_x), pitch rate (ω_y), and yaw rate (ω_z).

$$M_x = \dot{\omega}_x I_1 - \omega_y \omega_z I_2 + \omega_y \omega_z I_3 \quad (1)$$

The advancement of automobile dynamics controls has shifted its attention to the roll angle as a predictor of an imminent rollover accident due to the growing safety regulations for passenger cars in recent times [3]. By shifting the car's weight to one side, body roll lessens the force applied to the tires on the other side of the vehicle. This may result in decreased grip and traction, which would make it harder for the car to stay under control when making fast turns. The car may become unstable due to excessive body roll, which increases the risk of oversteering—the back end sliding out—or understeering—the front end losing traction. This may make controlling the vehicle more challenging, particularly in situations involving racing or high-performance driving [4].

The rollover of a vehicle is one of the most severe types of accidents on the road that can have devastating consequences for both the driver and the passenger of the vehicle, as well as bystanders and pedestrians. There are several factors that influence these events, including the dynamics of the vehicle, road conditions, and the behavior of the driver. Figure 2 [5] illustrates the fatalities resulting from rollover crashes from 2011 to 2020 for different types of vehicles, with over 7000 casualties reported in 2020 alone. Rollover crashes were identified as the most lethal type of incident involving passenger vehicles that year, contributing to 30% of all human fatalities. This research was undertaken with the aim of mitigating these figures and enhancing safety measures.

Over the years, research has been conducted regarding the roll induced in a vehicle. Ervin [6] examined the effect of the vehicle size and weight on the roll induced. Digges et al. [7] investigated how the speed of the vehicle influenced the rollover in a vehicle. Ryu and Gerdes [8] introduced a method to use the Global Positioning System [GPS] and Inertial Navigation System [INS] sensors to determine the roll induced in a vehicle on a banked road. Kar et al. [9] introduced a better measure for the relative roll instability in a vehicle: Normalized Roll-response of Semitrailer Sprung Mass. This measure is based on the normalized roll response of the sprung and unsprung masses, which was measured online. Parent et al. [10] simulated the rollover induced in vehicles and researched the effect of the stiffness of the vehicle body on the roll of the vehicle. Seyedi et al. [11] conducted a detailed study on rollover crashes induced in passenger vehicles and researched the parameters that affect them. Many methods to record the roll induced have also been researched. Papaioannou et al. [12] conducted a sensitivity analysis examining how the roll center of a vehicle affects both its performance and ride comfort.

Various methods are used to reduce the roll induced in the vehicle. Using five distinct suspension systems, Cole [13] has conducted a numerical (modeling) assessment of the roll dynamics of heavy trucks. The study analyzes several active and passive suspension systems and concludes that ride comfort may be

*Corresponding author: Zeinab El-Sayegh, Department of Automotive and Mechatronics Engineering, Ontario Tech University, Canada. Email: zeinab.el-sayegh@ontariotechu.ca

Figure 1
Forces acting on a turning vehicle

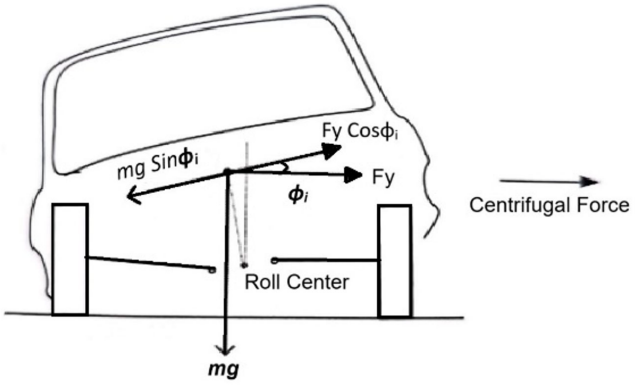

Figure 2
Rollover fatalities in different vehicles (2011–2020)

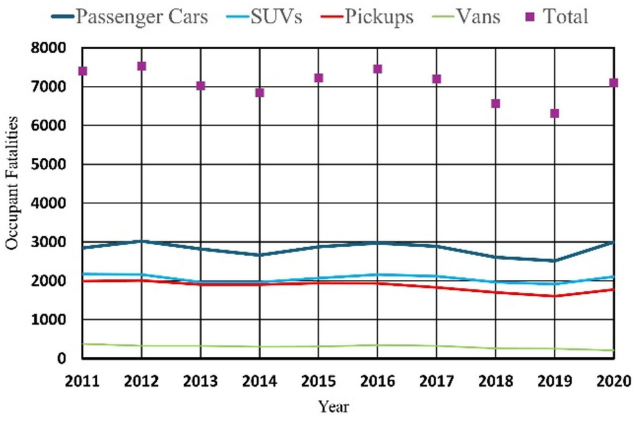

sacrificed in order to raise an anti-roll bar's rigidity and improve a vehicle's roll stability. Cao et al. [14] and Cao et al. [15] conducted tests using hydro-pneumatic suspensions. The results indicate that they provide significant advantages in terms of increased anti-roll and anti-pitch characteristics, as well as improved ride and handling performance, all in a flexible and energy-efficient way. Nikyar et al. [16] developed an active warning system and an active braking system aimed at preventing rollovers in all-terrain vehicles. Hou et al. [17] designed a "Model Predictive Control" controller which allowed a vehicle to operate at higher speeds while avoiding rollovers. Yim et al. [18] utilized two extended Kalman filters (EKFs)—a state estimator and a parameter estimator—and validated their dual EKF approach through simulations and experiments, demonstrating its efficacy in enhancing active roll control. Elliott et al. [19] patented a Predictive Functional Control system that adjusts vehicle dynamics in real-time, gyroscopic sensors that monitor roll angles, and deploys anti-rollover devices that provide additional stability during rollovers.

This study investigates the use of wheel spacers. They are attached to wheel hubs to widen the vehicle's wheelbase and to fit tires when the bolt pattern on the wheels and the hub differ [20]. Figure 3 [21] depicts an example of the schematic of a wheel spacer. They accommodate differing bolt patterns and enhance stability on curves, albeit with potential drawbacks like increased

Figure 3
Schematic diagram of a wheel spacer

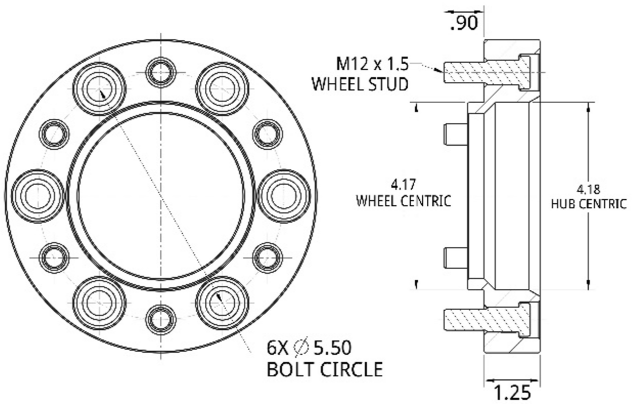

hub stress. Wheel spacers improve handling by widening the wheelbase, boosting grip, and reducing the risk of rollovers. A vehicle with a wider wheelbase has a better chance of preventing a rollover [22]. They also address misalignments and provide room for modifications like larger brakes or wider wheels. Cost-effective and readily available, wheel spacers offer an easy solution for widening the wheelbase.

As illustrated in the literature study above, although the research to prevent rollover was vast, most of it was done using active devices. Research to prevent rollover using passive devices was very few. To the best of the authors' knowledge, the prevention of rollover using wheel spacers is a novel study.

2. Methodology

The research utilized the CarSim modeling and Simulation software [23] selected for its self-contained nature, extensive library, and integrated controllers that facilitate a range of tests. The CarSim modeling software consists of a vast library of different-sized vehicle accurate models. Parameters of these vehicle models such as wheelbase, tires used, etc. can be easily modified. The software was operated on a computer system equipped with an AMD Ryzen 7 6800H processor, 16 GB of RAM, and a 64-bit operating system. Data obtained from the conducted tests were subsequently read, analyzed, and plotted using Microsoft Excel 2021.

Initially, relevant research was carried out to select the base vehicle model. This involved examining various options through an extensive review of journal articles and other publications. Given that the rollover probability of a vehicle is directly proportional to its speed and inversely proportional to the height of its center of gravity [24], we aimed to minimize the influence of these factors during the sensitivity analysis of wheel spacers on vehicle roll. Therefore, we selected a B-class sports car for this study, due to its high-speed capabilities and low center of gravity.

CarSim's user-friendly interface facilitated the methodology, making it relatively straightforward. Using the appropriate specifications, the base vehicle model was created. Subsequently, four different models of the vehicle were developed, which will be discussed in a later section. Once the designs were finalized, the models were subjected to two rollover stability tests: the fish hook test procedure and the Circular Road test procedure. The following sections delve into the details and specifications of these tests. After the tests were conducted, the data were exported

Figure 4
Methodology flowchart for CarSim model

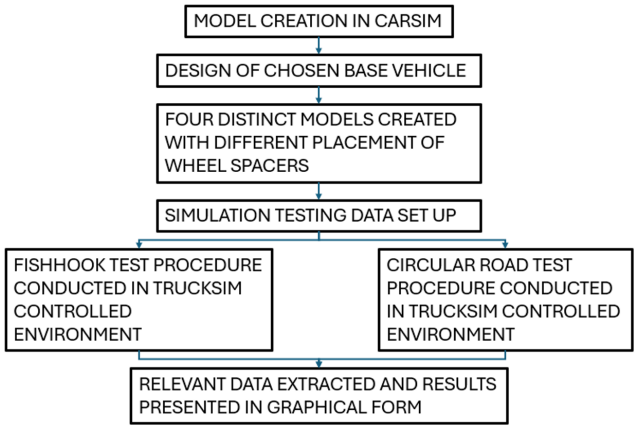

to Microsoft Excel for analysis and graphical presentation to illustrate the differences between the models. The results of this study are presented below. Figure 4 provides a flowchart illustrating the applied methodology.

3. Vehicle Model Specifications

As stated, a B-class sports car was selected for this study The Simulink diagram for the vehicle controller is depicted in Figure 5. The vehicle is a two-wheel drive vehicle with its rear axle experiencing the engine torque. The spring mass was 1020 kg with its length and width being 3300 mm and 1718 mm, respectively. The sports car was 1080 mm high with a ground clearance of the vehicle being 330 mm in the front and 310 mm at the back. The vehicle is powered by an internal combustion diesel engine providing 150 kw of power. The internal transmission powertrain was a 6-speed control with a gear ratio of 4.1:1. All the parameters, including those previously mentioned, are standardized parameters obtained from the software library.

The distance between the two axles was 2330 mm with the center of gravity of the vehicle 1165 mm behind the front axle. The sports car had a built-in ABS control system in it. The vehicle was also equipped with a power steering mechanism. Each of the four wheels had a Kingpin inclination of 8 degrees and a Castor Angle of 3.5 degrees. For the vehicle model with no

Figure 6
Width of axles with and without spacers

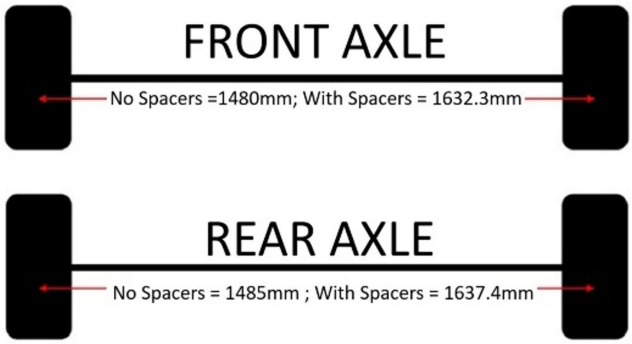

spacers, the distance between the centers of the front wheels was 1480 mm while the distance between the rear wheel centers was 1485 mm. The front wheels had a camber of −1 degree and a −0.2 degree toe angle. The rear axle had a −1.5 degree camber with a 0.2 degree toe angle. For this study, the sports car was equipped with 205/45 R17 tires.

The spacers considered in this study were 3-inch (76.2 mm) spacers. Four models were created for this study. Model 1 was the sports car with no spacers at either of its axles. This will be further referred to as "*No Spacer model.*" Model 2 is the vehicle with spacers on both axles (referred to as "*Both Spacer model*"). Model 3 is a model with only its front wheels being fitted with spacers while model 4 was only fitted with spacers on its rear wheels. For the remainder of this paper, these cases are going to be referred to as "*Front Spacer model"* and "*Rear Spacer model*" respectively. To replicate the effects of the spacer, the distance between the tires was changed in each case. Figure 6 depicts the width of the axles when the spacers are present and absent. With the spacers installed on both sides, the front axle has a width of 1632.4 mm while the rear axle has a width of 1637.4 mm. Without the spacers on either side, the front axle is 1480 mm wide and the rear axle is 1485 mm wide.

4. Simulation Setup

The simulation was carried out using CarSim simulation and modeling software [23]. CarSim is the world's most established vehicle simulation platform. It delivers the most accurate, detailed,

Figure 5
Simulink diagram for 6-speed transmission vehicle

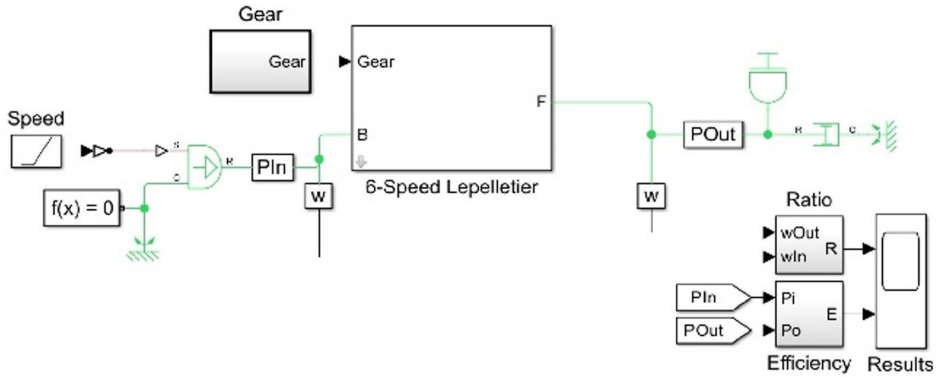

and efficient methods for simulating the performance of a variety of personal and commercial vehicles. It is widely used to analyze vehicle dynamics, develop active controllers, calculate a truck's performance characteristics, and engineer next-generation active safety systems.

In order to determine the handling characteristics, the models were subjected to two different tests as discussed in the sections below.

4.1. Fish hook test procedure

A fishhook test is a complete experiment that is used to evaluate the stability of the vehicle and its ability to avoid rollover [25]. It measures the vehicle's ability to follow a trail and avoid obstacles in emergency situations as well as what its roll stability limit is. It is therefore one of the worst circumstances under which to drive.

For the test, the vehicle was subjected to an initial speed of 80 kmph, with a steer input of 142.5 degrees applied in the left direction. The vehicle experiences a change of 712 deg/s and holds the steer angle for 0.4 s. This is followed by a second counter-steer angle of 285.14 degrees to bring the steer angle to −142.5 degrees. The steering angle is maintained for the remainder of the test. Table 1 summarizes the parameters used for the test. These parameters were chosen because they were the standard parameters for the fish hook test procedure in CarSim Simulation software. Figure 7 shows a visual depiction of the change of steering wheel angle with time elapsed. From the test, the vertical forces (*Fz*) acting on the vehicle axles, the roll angle (Roll), the roll rate (*R*), and the auxiliary roll moment (*Mx*) on each axle were derived using simulation.

Table 1
Parameters for fish hook test procedure

Parameters	Unit	Value
The first ramp input angle	deg	142.57
Ramp input velocity	deg/s	712
Time held for first input	s	0.05
Time held for second input	s	3

Figure 7
Time rate of change of steering wheel angle

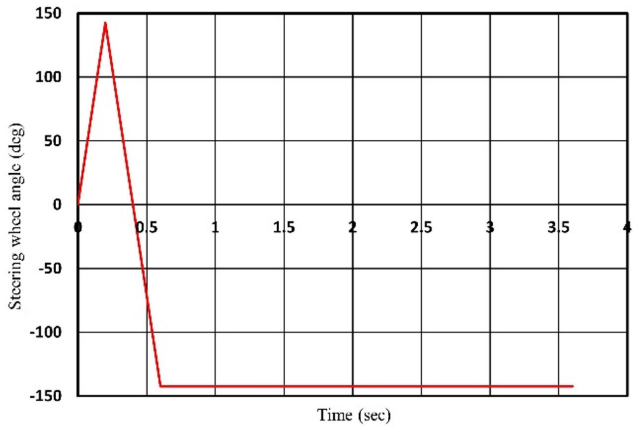

4.2. Turn on circular road

As the vehicle travels on a constant path, the vehicle experiences lateral forces due to the centrifuge effect. This lateral force develops a roll moment in the vehicle, prompting the vehicle to roll over. This test was chosen to simulate real-world driving conditions. The designated path to be followed by the vehicle is illustrated in Figure 8. There are a number of situations in which a vehicle and its user may experience this situation frequently.

Figure 8
Ideal path followed by vehicle

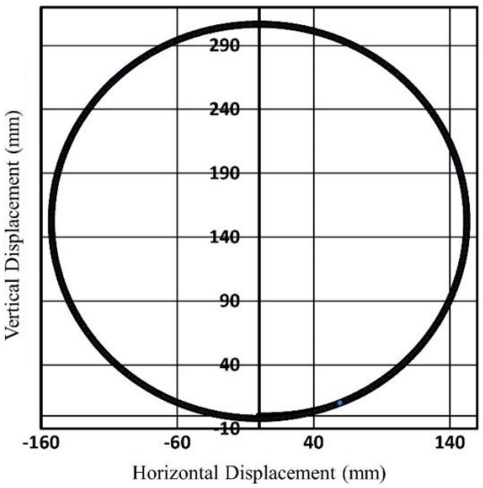

For this test, the vehicle was run on an asphalt road with coefficient of friction of 0.85. The path followed by the vehicle is circular. The turning radius of the vehicle is 152.4 m (500 feet). The constant speed the vehicle tried to maintain was 120 kmph. The test ran for 60 s. Table 2 summarizes the parameters used for the test. The speed was chosen (120 km/h) to replicate the speed limit on North American highways. The remaining parameters were standard parameters for the Circular Road test procedure in CarSim Simulation software The roll angle induced on each axle and the vehicle was the prime focus and the desired result of this simulation setup.

Table 2
Parameters for circular road test procedure

Parameters	Unit	Value
Initial speed of vehicle	m/s	33.33
Max Steer angle of vehicle	deg	36.66
Radius of turn	m	152.4
Time	s	60

5. Results and Discussion

The simulation results were exported to an Excel file. The data were sorted, and the required information was extracted. This was then depicted using line graphs in Microsoft Excel. For the following graphs, the red line depicts the results of the *No Axle model*, the blue line depicts the results of the *Both Axle model*, the green depicts the *Front Axle model,* and the yellow line depicts the *Rear Axle model* in all the tests.

5.1. Fish hook test procedure: Vertical forces acting on each axle

The results for the vertical forces acting on the front axle are depicted in Figure 9. The result for the vertical forces acting on

Figure 9
Vertical forces (*Fx*) acting on front axle

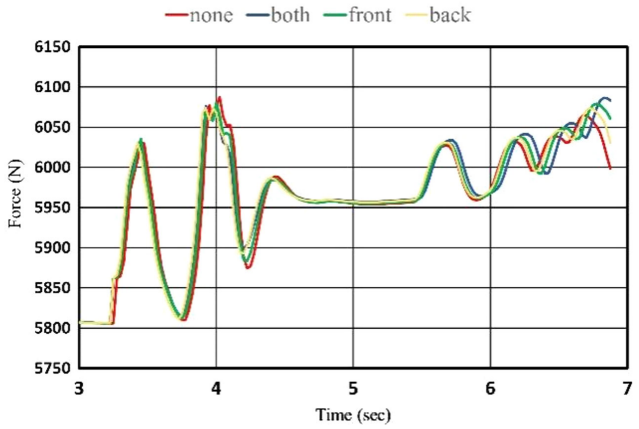

Figure 10
Vertical forces (*Fx*) acting on rear axle

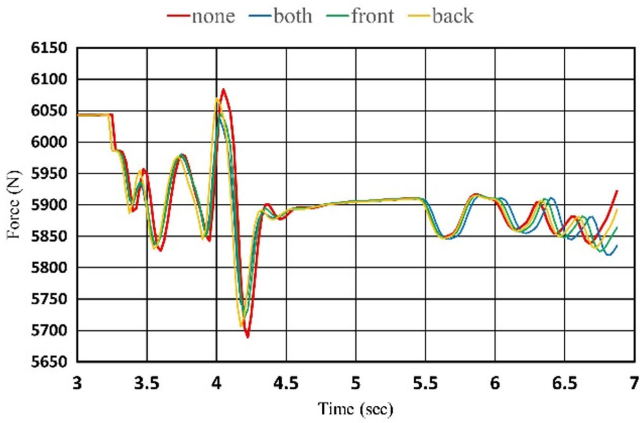

the rear axle is depicted in Figure 10. The graphs of the *No Spacer model* show the most variation in the vertical forces for both axles. Table 3 provides a summary of the findings pertaining to the forces acting on the front axle, while Table 4 presents the results concerning the rear axle.

Table 3
Vertical forces (*Fx*) acting on front axle in fish hook procedure

Model used	Max Fz (Nm)	Min Fz (Nm)	Range
No Spacer model	6087.42	5806.19	277.56
Both Axle model	6086.58	5815.39	271.19
Front Axle model	6080.51	5812.02	268.49
Rear Axle model	6074.33	5811.09	263.24

Table 4
Vertical forces (*Fx*) acting on rear axle in fish hook procedure

Model used	Max Fz (N)	Min Fz (N)	Range
No Spacer model	6083.87	5689.50	397.93
Both Axle model	6037.09	5733.80	352.77
Front Axle model	6044.93	5719.66	360.85
Rear Axle model	6070.32	5706.20	368.14

In terms of the vertical forces exerted on the front axle, the *No Spacer model* registered a peak force of 6087.42 N, whereas the *Both Spacer model* recorded 6086.58 N. The *No Spacer model* exhibited the lowest minimum vertical force on the front axle at 5689.5 N, compared to 5733 N exerted by the *Both Spacer model*. Additionally, the *Front Spacer model* demonstrated higher force than the *Rear Spacer model*. Toward the conclusion of the test, there is a significant increase in variation. The *Both Axle model* exhibits the greatest variation, followed by the *Front Axle model*, the *Rear Axle model*, and the *No Axle model*. At the end of the test, the forces peak at 6079.45 N, 6060.89 N, 6030.85 N, and 5973.66 N, respectively.

As for the forces acting on the rear axle, a similar trend is noticed. The *No Spacer model* experienced the most variations in the minimum and maximum values of forces while the *Both Spacer model* experienced the least. When the *Front Spacer model* with the *Rear Spacer model* is compared, it is evident that the former experiences a higher minimum force, whereas the latter endures a higher maximum force. Furthermore, each model exhibits a variation in forces towards the end of the test, with the *No Axle model* experiencing the highest force at the test's conclusion.

Overall, the front axle experiences more force than the rear axle in all the models, but the range of forces in every model was more in the rear axle.

5.2. Fish hook test procedure: Auxiliary roll moment on each axle

Figure 11 illustrates the roll moment acting on the front axle during the test. An illustration of the roll moment acting on the rear axle is in Figure 12. Every model follows a similar trend line with the difference being in peak values on both sides. This variation occurs when the steering in the vehicle is turned rapidly to the opposite side in the fish hook test. Table 5 summarizes the results of the test for the roll moment acting on the front axle while Table 6 summarizes the results of the test for the rear axle.

Discussing the roll moment on the front axle, the *No Spacer model* experiences the highest range with 813.59 Nm. This is 23% more than the range endured by the *Both Spacer model* (659.80 Nm). The *No Spacers model* displayed a maximum moment of 388.29 Nm on one side while having 425.31 Nm on the other. The *Both Spacer model* experiences the smallest peaks with 322.13 Nm and 337.62 Nm on either side, while the axle with both gave 5733 N. The Rear Spacer model outperformed the

Figure 11
Roll moment acting on the front axle

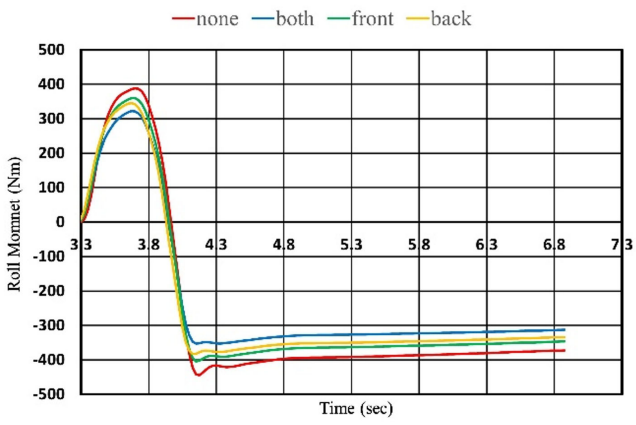

Figure 12
Roll moment acting on the rear axle

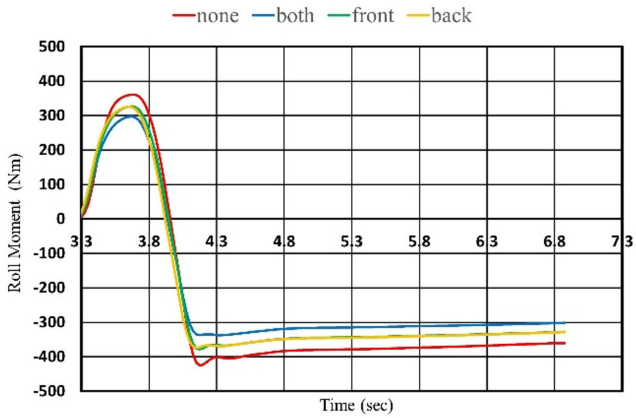

Figure 13
Roll acting on the vehicle

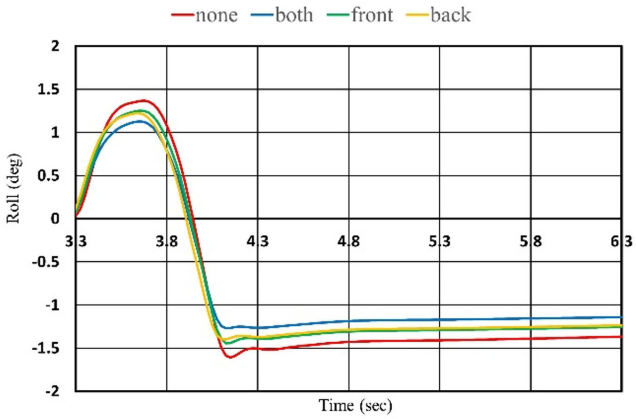

Table 5
Auxiliary moment (*Mx*) acting on front axle in fish hook procedure

Model used	Max *Mx* (Nm)	Min *Mx* (Nm)	Range
No Spacer model	388.27	−425.39	813.59
Both Axle model	322.14	−337.67	659.80
Front Axle model	359.48	−378.54	738.02
Rear Axle model	345.25	−374.50	719.74

Table 6
Auxiliary moment (*Mx*) acting on rear axle in fish hook procedure

Model used	Max *Mx* (Nm)	Min *Mx* (Nm)	Range
No Spacer model	360.73	−425.38	786.11
Both Axle model	296.96	−337.67	634.63
Front Axle model	326.84	−378.54	705.37
Rear Axle model	325.37	−374.50	699.87

Front Spacer model, characterized by a narrower range and lower peak values on both sides.

Like the front axle, the rear axle also experiences the most range on the *No Spacer model* (786.11 Nm) and the least on the *Both Spacer model* (634.63). The *Both Spacer model* shows reductions of 18% and 21% in maximum and minimum force peaks, respectively, compared to the *No Spacer model*. The *Front Spacer model* and the *Rear Spacer model* experience similar trajectories, with differences of 1.47 Nm and 4.04 Nm between their maximum and minimum force peaks, respectively.

5.3. Fish hook test procedure: Roll and roll rate of the vehicle

Figure 13 depicts the vehicle's roll during testing, while Figure 14 illustrates the vehicle's roll rate under the same conditions. Analysis of Figure 12 and Figure 13 reveals that the *No Spacer model* exhibits significantly greater roll and higher roll rates compared to all other vehicle configurations. Specifically, the difference in the roll rates (compared to the *Both Spacer model*) is notable, reaching 1 degree on one side and nearly 2 degrees on the other. In contrast, the *Both Spacer model* demonstrates the least roll and the most favorable roll rate among all tested models. Like the previous result, the *Rear Spacer model* and the *Front Spacer model* follow similar trajectories, with the roll rate slightly better in the *Front Spacer model*. The results for the roll and roll rate induced in the vehicle are summarized in Tables 7 and 8, respectively.

Figure 14
Roll rate experienced by the vehicle

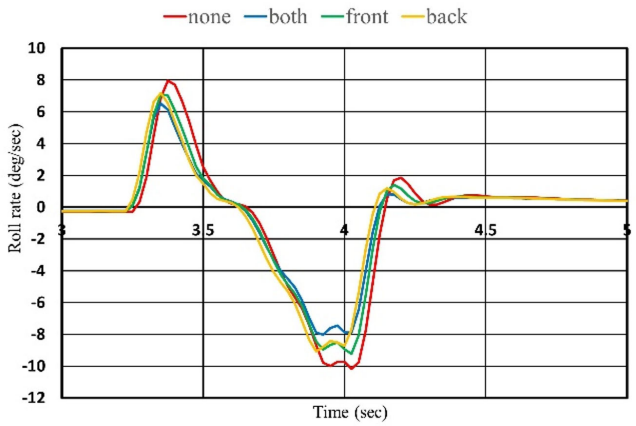

Table 7
Roll acting on the vehicle in the fish hook procedure

Model used	Max angle (deg)	Min angle (deg)	Range
No Spacer model	1.367	−1.610	2.977
Both Axle model	1.128	−1.267	2.398
Front Axle model	1.252	−1.441	2.694
Rear Axle model	1.222	−1.399	2.620

5.4. Circular road test procedure: Roll experienced by individual axles

Figures 15 and 16 illustrate the roll induced in the front and rear axle respectively, during the Circular Road Test procedure. Table 9

Table 8
Roll rate experienced by the vehicle in the fish hook procedure

Model used	Max rate (deg/s)	Min rate (deg/rate)	Range
No Spacer model	7.956	−10.157	18.113
Both Axle model	6.520	−8.023	14.544
Front Axle model	7.096	−9.227	16.233
Rear Axle model	7.183	−9.062	16.245

Figure 15
Roll experienced by the front axle

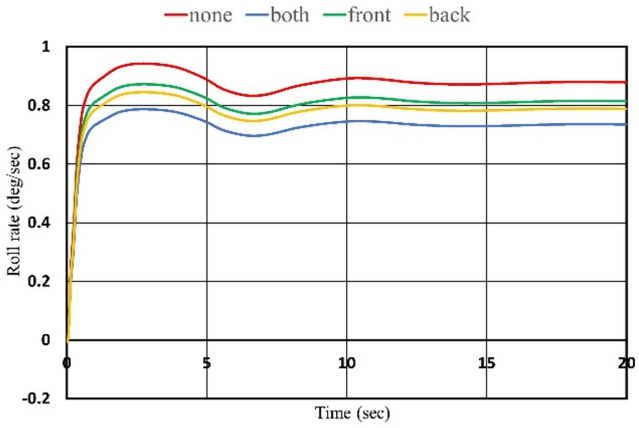

Figure 16
Roll experienced by the rear axle

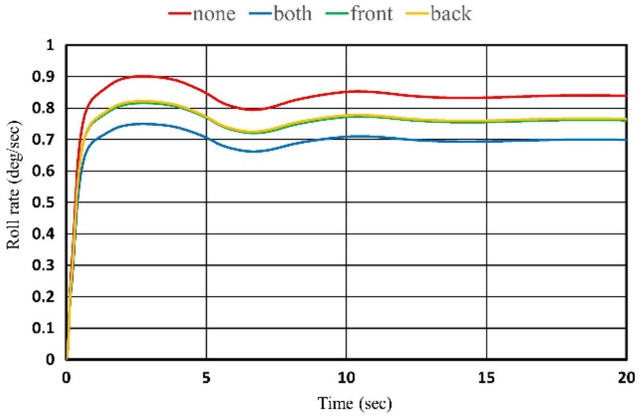

Table 9
Roll acting on the front axle in curved road test

Model used	Max angle (deg)
No Spacer model	0.943
Both Axle model	0.787
Front Axle model	0.872
Rear Axle model	0.845

Table 10
Roll acting on the rear axle in curved road test

Model used	Max angle (deg/s)
No Spacer model	0.901
Both Axle model	0.749
Front Axle model	0.816
Rear Axle model	0.822

depicts the roll acting on the front axle in every spacer orientation while Table 10 shows the roll acting on the rear axle in every orientation.

In the depicted figures, the roll characteristics of the *Both Spacer model*, *No Spacer model*, *Front Spacer model*, and *Rear Spacer model* reveal distinct patterns. Specifically, the *Both Spacer model* exhibits the least roll induced on both its front and rear axles compared to the *No Spacer model*, which experiences the highest roll on both axles. Upon commencement of the turn, the roll experienced by each axle exhibits initial variability. However, after a duration of 10 s, the roll stabilizes and maintains a consistent level thereafter.

Additionally, the *Front Spacer model* exhibits a marginally higher roll on the front axle, with an increase of 0.27 degrees compared to the *Rear Spacer model*. The graphs for the rear axle appear similar, with the *Rear Spacer model* demonstrating a slight advantage over the *Front Spacer model* by 0.06 degrees at its peak.

5.5. Circular road test procedure: Roll experienced by vehicle

Figure 17 illustrates the roll experienced by the vehicle model during the Circular Road test simulation. It is evident from the figure that the roll induced in the *Both Spacer model* was the lowest, being 20% less than that in the *No Spacer model*. Specifically, the *No Spacer model* exhibited a peak roll of 1.289 degrees, whereas the *Both Spacer model* had a maximum roll of 1.069 degrees. Additionally, when comparing the *Front Spacer model* to the *Rear Spacer model*, the *Front Spacer model* performed slightly better, with a peak roll difference of 0.015 degrees between the two. The trajectories for both models were found to be similar. Table 11 presents the maximum roll values for each model.

Figure 17
Roll experienced by the vehicle

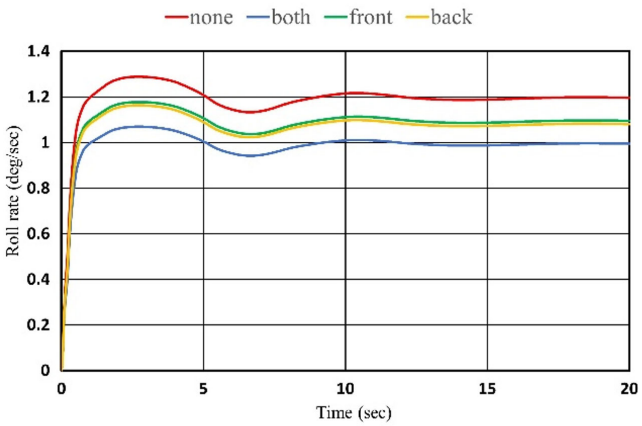

Table 11
Roll experienced by vehicle in curved road test

Model used	Max angle (deg)
No Spacer model	1.289
Both Axle model	1.069
Front Axle model	1.178
Rear Axle model	1.163

6. Conclusion

The Fishhook tests demonstrated a clear correlation between the introduction of spacers and an increase in the moment exerted on the axles. This is in accordance with the fact that the moment is a product of the Force applied [in this case the lateral force on the wheels] and the perpendicular distance from the point [the distance being half the width of the wheelbase] [26]. This is due to the fact that the individual forces acting on the axle favored the *No Spacer model*. When comparing the models with spacers on either axle, the *Rear Axle model* induced more vertical forces in both its axles. Also, upon further comparison, introducing the spacers only in the front axle [*Front Axle model*] generated a greater moment in both the axles.

The roll and roll moment of the vehicle in all the tests favored the model with the spacers on all its wheels [*Both Axle model*]. This is due to the fact that as the width of the car increases, so does the moment required to turn it over. Even though the moment induced in the *Both Axle model* was much more than the rest, it displayed the least rollout of the rest.

Upon analyzing the *Front Spacer model* and the *Rear Axle model* separately, the roll experienced by the vehicle was the worst when the spacers were installed only on the front axle [*Front Axle model*] in both tests. Although installing spacers exclusively on one axle is not recommended, if a choice must be made, installing them on the rear axle would be the better solution for this vehicle.

With this study, we can conclude that the roll experienced by the vehicle can be decreased by the addition of spacers in all its wheels. All tests indicate that the roll and roll rate is 20% less with spacers installed. However, due to the fact that the spacer wheels induced more vertical force on the wheels, this compromises the life of all the components attaching the wheels to the body of the vehicle.

Recommendations

The study concluded that wheel spacers can effectively reduce the roll experienced by the vehicle. The notion of evaluating the capacity of wheel spacers to diminish vehicle roll is novel. An inherent limitation of this study is its failure to consider the potential adverse impacts that the spacers may exert on the structural integrity of the vehicle's chassis. To address the limitation, future research should include a thorough structural analysis and testing of the spacers in various operational scenarios. This could involve finite element analysis to simulate stress and strain on the chassis with the spacers installed, as well as real-world durability testing under different load conditions. Additionally, incorporating feedback from automotive engineers and conducting a comparative study with vehicles not using spacers could provide valuable insights into any potential structural compromises.

This study focused on a passenger sports car, chosen for its typically lower center of gravity. Future research should extend to vehicles with a higher center of gravity, such as trucks, pickups, and SUVs, to explore variations in center of gravity height.

Furthermore, considering the rising number of rollover incidents due to collision avoidance, future studies should investigate the effects of spacers using the Moose test. This evasive maneuver test assesses a vehicle's ability to evade unexpected obstacles. This test will give a better understanding of a vehicle's collision avoidance capabilities.

Addressing these research gaps is essential for advancing our understanding and developing more effective solutions to enhance the roll stability of vehicles by utilizing passive devices such as wheel spacers.

Ethical Statement

This study does not contain any studies with human or animal subjects performed by any of the authors.

Conflicts of Interest

The authors declare that they have no conflicts of interest to this work.

Data Availability Statement

Data available on request from the corresponding author upon reasonable request.

Author Contribution Statement

Glenn Xavier Vaz: Conceptualization, Methodology, Software, Validation, Formal analysis, Investigation, Resources, Data curation, Writing – original draft, Writing – review & editing, Visualization; **Zeinab El-Sayegh:** Conceptualization, Formal analysis, Resources, Writing – original draft, Writing – review & editing, Visualization, Supervision, Project administration, Funding acquisition.

References

[1] Ahmad, E., & Youn, I. (2023). Performance improvement during attitude motion of a vehicle using aerodynamic-surface-based anti-jerk predictive controller. *Sensors*, *23*(12), 5714. https://doi.org/10.3390/s23125714

[2] Jazar, R. N. (2019). Vehicle roll dynamics. In R. N. Jazar (Ed.), *Advanced vehicle dynamics* (pp. 215–296). Springer. https://doi.org/10.1007/978-3-030-13062-6_3

[3] Rehm, A. (2010). Estimation of vehicle roll angle. In *4th International Symposium on Communications, Control and Signal Processing,* 1–4. https://doi.org/10.1109/ISCCSP.2010.5463458

[4] Wong, J. Y. (2022). *Theory of ground vehicles*. USA: Wiley.

[5] Schubert, A., Babisch, S., Scanlon, J. M., Campolettano, E. T., Roessler, R., . . . , & McMurry, T. L. (2023). Passenger and heavy vehicle collisions with pedestrians: Assessment of injury mechanisms and risk. *Accident Analysis & Prevention*, *190*, 107139. https://doi.org/10.1016/j.aap.2023.107139

[6] Ervin, R. D. (1986). The dependence of truck roll stability on size and weight variables. *International Journal of Vehicle Design*, *7*(5–6), 192–208.

[7] Digges, K. H., Malliaris, A. C., Ommaya, A. K., & McLean, J. (1991). Characterization of rollover casualties. In *Proceedings of the International IRCOBI Conference on the Biomechanics of Impacts,* 309–319. https://hdl.handle.net/2440/48676

[8] Ryu, J., & Gerdes, J. C. (2004). Estimation of vehicle roll and road bank angle. In *Proceedings of the 2004 American Control Conference,* 2110–2115. https://doi.org/10.23919/ACC.2004.1383772

[9] Kar, S., Rakheja, S., & Ahmed, A. K. W. (2006). A normalised measure of relative roll instability for open-loop rollover

warning. *International Journal of Heavy Vehicle Systems*, *13*(1–2), 74–97.

[10] Parent, D. P., Kerrigan, J. R., & Crandall, J. R. (2011). Comprehensive computational rollover sensitivity study, part 1: Influence of vehicle pre-crash parameters on crash kinematics and roof crush. *International Journal of Crashworthiness*, *16*(6), 633–644. https://doi.org/10.1080/13588265.2011.616114

[11] Seyedi, M., Jung, S., Wekezer, J., Kerrigan, J. R., & Gepner, B. (2020). Rollover crashworthiness analyses – An overview and state of the art. *International Journal of Crashworthiness*, *25*(3), 328–350. https://doi.org/10.1080/13588265.2019.1593290

[12] Papaioannou, G., Gauci, C., Velenis, E., & Koulocheris, D. (2020). Sensitivity analysis of vehicle handling and ride comfort with respect to roll centers height. In *Advances in Dynamics of Vehicles on Roads and Tracks: Proceedings of the 26th Symposium of the International Association of Vehicle System Dynamics*, 1730–1739. https://doi.org/10.1007/978-3-030-38077-9_197

[13] Cole, D. J. (2000). Evaluation of design alternatives for roll-control of road vehicles. In *Proceedings of 5th International Symposium on Advanced Vehicle Control, AVEC 2000,* 561–567.

[14] Cao, D., Rakheja, S., & Su, C. Y. (2010). Roll-and pitch-plane coupled hydro-pneumatic suspension: Part 1: Feasibility analysis and suspension properties. *Vehicle System Dynamics*, *48*(3), 361–386. https://doi.org/10.1080/00423110902883251

[15] Cao, D., Rakheja, S., & Su, C. Y. (2010). Roll-and pitch-plane-coupled hydro-pneumatic suspension: Part 2: Dynamic response analyses. *Vehicle System Dynamics*, *48*(4), 507–528. https://doi.org/10.1080/00423110902923461

[16] Nikyar, E., Venkatachalam, V., & Drugge, L. (2020). Designing and evaluating active safety systems for rollover prevention of all-terrain vehicles. In *Advances in Dynamics of Vehicles on Roads and Tracks: Proceedings of the 26th Symposium of the International Association of Vehicle System Dynamics*, 989–999. https://doi.org/10.1007/978-3-030-38077-9_115

[17] Hou, Y., Xiong, L., Leng, B., & Yu, Z. (2020). Integrated control for four-wheel-independent-drive EVs' lateral stability and rollover prevention. In *Advances in Dynamics of Vehicles on Roads and Tracks: Proceedings of the 26th Symposium of the International Association of Vehicle System Dynamics,* 1333–1341. https://doi.org/10.1007/978-3-030-38077-9_154

[18] Yim, S., Nah, J., & Park, M. (2020). Estimation of states and parameters with dual extended Kalman filters for active roll control. In *Advances in Dynamics of Vehicles on Roads and Tracks: Proceedings of the 26th Symposium of the International Association of Vehicle System Dynamics,* 1616–1623. https://doi.org/10.1007/978-3-030-38077-9_184

[19] Elliott, T., Ramey, M., Ramey, V., & Ramey, A. (2023). *Vehicle anti-rollover device and method*. Retrieved from: https://patents.google.com/patent/US20230249638A1/en

[20] Prasad, N., Pradeep, H., & George, A. M. (2017). Modelling and static analysis of wheel spacer. *International Journal of Engineering Research & Technology*, *6*(2), 217–222.

[21] Spidertrax. (2024). *Toyota 1.25" thick wheel spacers [Review of Toyota 1.25" thick wheel spacers]*. Retrieved from: https://www.spidertrax.com/whs023

[22] Tragakis, C. J. (2024). *What are wheel spacers?* Retrieved from: https://www.cjponyparts.com/resources/what-are-wheel-spacers?srsltid=AfmBOorrK9F2F8vg4Q-RJE8MIsmxKq6YUN38OiZy9e_o_7bX0pT4OU_x

[23] CarSim. (n.d.). *Mechanical simulation*. Retrieved from: https://www.carsim.com/products/carsim/

[24] Huston, R. L., & Kelly, F. A. (2014). Another look at the static stability factor (SSF) in predicting vehicle rollover. *International Journal of Crashworthiness*, *19*(6), 567–575. https://doi.org/10.1080/13588265.2014.919730

[25] Xiong, F., Lan, F., Chen, J., & Zhou, Y. (2015). The study for anti-rollover performance based on fishhook and J turn simulation. In *Proceedings of the 3rd International Conference on Material, Mechanical and Manufacturing Engineering,* 2084–2093. https://doi.org/10.2991/ic3me-15.2015.401

[26] Rajamani, R. (2011). *Vehicle dynamics and control*. Germany: Springer.

How to Cite: Vaz, G. X., & El-Sayegh, Z. (2024). Analysis of the Effects of Wheel Spacers on the Roll Stability of the Vehicle. *Archives of Advanced Engineering Science*. https://doi.org/10.47852/bonviewAAES42023106